Fuel 224 (2018) 637–643

Contents lists available at ScienceDirect

Fuel

journal homepage: www.elsevier.com/locate/fuel

Full Length Article

Model-free adaptive control for MEA-based post-combustion carbon capture processes

Ziang Li[a], Zhengtao Ding[a,*], Meihong Wang[b], Eni Oko[b]

[a] School of Electrical and Electronic Engineering, University of Manchester, Manchester M13 9PL, UK
[b] Department of Chemical and Biological Engineering, University of Sheffield, Sheffield S1 3JD, UK

ARTICLE INFO

Keywords:
Post-combustion carbon capture
Process control
Model-free adaptive control
System identification
Neural networks

ABSTRACT

For the flexible operation of mono-ethanol-amine-based post-combustion carbon capture processes, recent studies concentrate on model-based protocols which require underline model parameters of carbon capture processes for controller design. In this paper, a novel application of the model-free adaptive control algorithm is proposed that only uses measured input-output data for carbon capture processes. Compared with proportional-integral control, the stability of the closed-loop system can be easily guaranteed by increasing a stabilizing parameter. By updating the pseudo-partial derivative vector to estimate a dynamic model of the controlled plant on-line, this new protocol is robust to plant uncertainties. Compared with model predictive control, tuning tests of the protocol can be conducted on-line without non-trivial repetitive off-line sensitivity or identification tests. Performances of the model-free adaptive control are demonstrated within a neural network carbon capture plant model, identified and validated with data generated by a first-principle carbon capture model.

1. Introduction

1.1. Background

Power generation from fossil fuel combustion is the single largest contributor of CO_2 emission [1]. The mono-ethanol-amine (MEA)-based post-combustion carbon capture (PCC) [2] technology is feasible for the large-scale CO_2 absorption since it can be achieved with relative simple retrofits of conventional fossil-fuel power plants [3]. To compensate load variations, for instance, due to intermittent renewable power sources, a fossil-fuel power plant usually supplies flexible power generation and sometimes serves as a swing generator for the power network. These inevitably cause fluctuations of the emitted flue gas flow rate and the mass fraction of CO_2 in the flue gas which are external disturbances [4] of the MEA-based PCC process and deteriorate model-based control performances. A control protocol for the process must be robust when confronting these uncertainties. Furthermore, for a tight CO_2 emission target [4] or a time-variant CO_2 allowance market condition [5], the plant controller should be appropriately designed such that the closed-loop system has fast responses.

1.2. Literature review

Previous studies of MEA-based PCC processes concentrated on proportional-integral (PI) control [4,6,7] with the relative gain array pairing strategy. Due to the optimality and flexibility requirements, recently, model predictive control (MPC) is implemented for the processes [8,9]. This model-based method is more appreciated since its optimality leads to faster responses or lower energy consumption according to a diverse range of the real-time objectives or scheduled load variations of a power plant. Although a dynamic PCC model [1] can be constructed in terms of the rigorous rate-based approach considering both chemical and physical properties, such a first-principle model is too complicated for the model-based control [10,11]. An identified model serving as the underline model is imperative to reduce the model complexities while ensure the model-based control performances. Previous studies focused on the optimal operation of the model-based control such as MPC but paid little attention to system identification before implementing such a control protocol. On the other hand, when the PCC process operation is coupled with a power plant [4], uncertain conditions of the power plant may degrade dynamic performances of the carbon capture facilities. For instance, fluctuations of either the flue gas flow rate or the CO_2 mass fraction in the flue gas, dependent on the power plant load conditions, will change the operating point of the PCC process. These disturbances cause extra mismatches between the model and the controlled non-linear PCC plant, which is classified as model uncertainties. A large number of sensitivity [6] or identification [12] tests for different operating points of the controlled plant must be

* Corresponding author.
E-mail address: zhengtao.ding@manchester.ac.uk (Z. Ding).

https://doi.org/10.1016/j.fuel.2018.03.096
Received 11 December 2017; Received in revised form 8 March 2018; Accepted 13 March 2018
Available online 30 March 2018
0016-2361/

conducted before the controller can be properly tuned and implemented on-line. It makes the model-based controller design a non-trivial issue.

1.3. Aim of the paper and its novelties

In this paper, a novel model-free adaptive control (MFAC) protocol [13,14] is applied to a non-linear MEA-based PCC plant model identified based on a validated neural network model using the validated data [15] generated by a first-principle model. Compared with PI control using predefined tuning parameters around fixed operating points, MFAC uses compact form dynamic linearisation (CFDL) or partial form dynamic linearisation (PFDL) to form a time-variant PCC model on-line, inferring that the model adapts to plant operating point changes. Compared with the model-based protocol which requires non-trivial sensitivity or identification tests to determine a model for off-line tuning before on-line implementation, MFAC has a simpler tuning procedure. The identified PCC model is only used for the initial off-line tuning. Thereafter, the tuning parameters can be flexibly retuned on-line with the measured input–output data of the controlled non-linear PCC plant. No model parameters identified off-line are required on-line. The underline model parameters, however, are essential for model-based protocols. They are used to ensure the stability and performances of the closed-loop system, inferring a complex and repetitive off-line tuning procedure. PI control requires no underline model parameters same as MFAC, but its stability analysis is based on models. MFAC can easily guarantee stability by a stabilizing parameter.

1.4. Outline of the paper

This paper is organized as follows. Firstly, the system identification problem is discussed to build a validated non-linear PCC model with a neural network structure using the data generated by a first-principle model. Secondly, compared with generalized predictive control (GPC), MFAC is designed based on an iterative algorithm including on-line linear model update, control policy update and a reset rule. Thirdly, with the identified PCC model serving as the controlled non-linear plant, simulation results of MFAC are presented compared with PI control and GPC. Conclusions are given in the end.

2. Model development

2.1. Dynamic modelling of the post-combustion carbon capture process

The first-principle dynamic model of the PCC process in this paper has been developed in gPROMS® with the rate-based approach using the design and operation specifications in [17]. All the reactions in PCC are assumed to attain equilibrium. Validation of this model was made using data of pilot plants [4,15]. The flow diagram (Fig. 1) shows the flue gas is initially fed into the bottom of the absorber while the lean MEA solution is injected from the top. After chemical reactions between CO_2 and the lean MEA countercurrently in the column, the purified gas with less CO_2 is vented to the atmosphere while a carbon-rich MEA solution is pumped into the downstream lean/rich cross heat exchanger and exchanges energy with the lean solution from the stripper. The stripper has the analogous structure as the absorbers. The pre-heated rich MEA from the exchanger outlet is pumped to the upper-stage and heated up when flowing down through the column. The heat is provided via a reboiler which separates CO_2 from the rich MEA and reproduces the lean MEA to process the consecutively discharged flue gas. Although a rigorous model can be built considering chemical reactions, it is too complex for control design [10]. A feasible mathematical model must be identified [8].

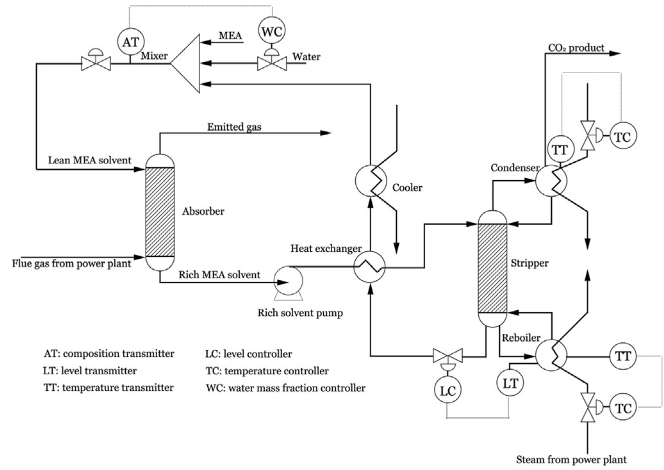

Fig. 1. The process flow diagram of a PCC plant [16].

2.2. Identification of neural networks for dynamic carbon capture processes

For the PCC process which is complex and non-linear, neural networks [18,19] can be selected to identify mathematical models based on off-line data generated by the above first-principle model. Note that the tracking problem of the carbon capture level is primarily considered in Section 3. For brevity, the lean loading and the re-boiler temperature are assumed to be fixed around 0.28 mol/mol and 387 K, respectively, for all cases in the later simulations. On that basis, a model related to the carbon capture level dynamics is built with three inputs and one output. The three inputs are the flue gas flow rate (kg/s), $d_1(t)$, mass fraction of CO_2 in the flue gas, $d_2(t)$ and the lean MEA flow rate (kg/s), $u(t)$, respectively. The output is the CO_2 or carbon capture level (%), denoted by $y(t)$. The candidate models of this process are neural networks with one hidden layer. Referring to Fig. 2, the model structure is represented by

$$\hat{y}(t+1) = \mathbf{w}^T\mathbf{z}(\mathbf{x}(t)) + b_o \tag{1}$$

where $\hat{y}(t+1)$ is the estimated capture level of the carbon capture process at time $t+1$; $\mathbf{w} = (w_1, w_2, ..., w_H)^T \in \mathbb{R}^H$ and $b_o \in \mathbb{R}$ are the weight vector and the bias, respectively, between the hidden and output layers; and $\mathbf{x}(t) \in \mathbb{R}^n$ is the input features at time t and defined as

$$\begin{aligned}\mathbf{x}(t) &\triangleq (x_1(t), x_2(t), ..., x_n(t))^T\\ &= (y(t), y(t-1), ..., y(t-n_a+1), d_1(t), d_1(t-1), ..., d_1(t-n_{d1}+1), d_2(t), d_2(t-1), ..., d_2(t\\ &\quad -n_{d2}+1), u(t), u(t-1), ..., u(t-n_b+1))^T\end{aligned}$$

with $n = n_a + n_b + n_{d1} + n_{d2}$. n_a, n_b, n_{d1}, and n_{d2} are model orders which must be determined in terms of model performances. $\mathbf{z}(\mathbf{x})$ is the output of the hidden layer, i.e., $\mathbf{z}(\mathbf{x}) \triangleq (z_1, z_2, ..., z_H)^T = g(\mathbf{V}\mathbf{x} + \mathbf{b}) \in \mathbb{R}^H$ with $g(\cdot)$ being an element-wise activation function for each entry of $\mathbf{V}\mathbf{x} + \mathbf{b}$ where $\mathbf{V} \in \mathbb{R}^{H\times n}$ and $\mathbf{b} \in \mathbb{R}^H$ are the weight matrix and the bias vector, respectively, between the input layer and hidden layer. Without losing generality, for $h \in \mathbb{R}$, the scalar activation function is logistic, i.e., $g(h) = 1/(1+\exp(-h))$. For a specific candidate model based on neural networks, the model parameters are weights $(\mathbf{w}, \mathbf{V})$ and biases $(b_o, \mathbf{b})$ which should be identified using the input and output data from the first-principle model. The total number of model parameters including weights and biases for the above neural network is $D = [(n+2)\cdot H] + 1$. To avoid overfitting [20], for two candidate models with similar model validation performances, the model with less complexity, i.e., smaller D, is preferred.

2.3. Model order selection with AIC

Akaike's information criterion (AIC) is used to determine the number of model parameters D_0. For a candidate model, i.e., the model structure (Eq. (1)) with a specific hidden layer size H and model orders, the residual is defined as the difference between the observation and

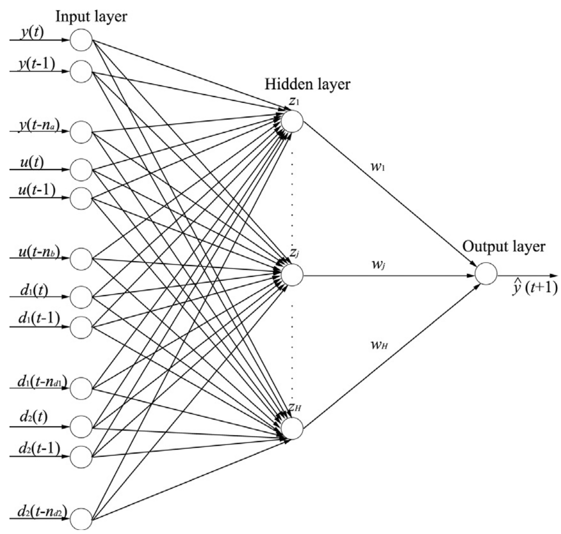

Fig. 2. A multi-input–single-output neural network with one hidden layer.

the one-step-ahead prediction of the output, which is $\epsilon(t) = y(t) - \hat{y}(t)$. $y(t)$ is the observed capture level of PCC processes. On that basis, the AIC value is estimated by $\text{AIC} = \ln(\hat{\sigma}^2) + 2D_0/N$ with $\hat{\sigma}^2 = (1/N)\sum_{t=1}^{N}\epsilon(t)^2$ where $\hat{\sigma}$ is an estimate of the noise standard deviation σ; N is the number of data samples; and $D_0 = D + 1$ is the number of model parameters including σ. In practice, the model orders may not be exactly selected by AIC. Residual analysis is used to validate the candidate models.

2.4. Residual analysis

The residual analysis [12] suggests a validated model has residuals $\epsilon(t)$ which are serially independent and unrelated to past inputs. Two correlation-based intermediate variables are defined as $\hat{R}_{\epsilon}^{N}(\tau) = (1/N)\sum_{t=1}^{N}\epsilon(t)\epsilon(t-\tau)$ and $\hat{R}_{\epsilon u}^{N}(\tau) = (1/N)\sum_{t=1}^{N}\epsilon(t)u(t-\tau)$. $\zeta_1(\tau)$ and $\zeta_2(\tau)$ are then defined as $\zeta_1(\tau) = (N/\hat{\sigma}^4)\cdot(\hat{R}_{\epsilon}^{N}(\tau))^2 \sim \chi^2(1)$ and $\zeta_2(\tau) = \sqrt{N/\hat{\sigma}^2 P(\tau)}\hat{R}_{\epsilon u}^{N}(\tau) \sim \mathcal{N}(0,1)$ with $P(\tau) = (1/N)\sum_{t=1}^{N}u(t-\tau)^2$. For a validated model, $\zeta_1(\tau)$ and $\zeta_2(\tau)$ should be within the α-level confidence intervals determined by the chi-squared- and normally-distributed random variables, respectively.

3. Model-based and model-free control protocols

The tracking problem of the carbon capture level $y(t)$ for the controlled non-linear PCC plant is considered in this section. The manipulated input is the lean MEA flow rate $u(t)$ [4,6]. The disturbances are the flue gas flow rate (kg/s) $d_1(t)$ and the mass fraction of CO_2 in the flue gas $d_2(t)$. Two possible protocols are discussed. One is model-based, called GPC; the other is MFAC. MFAC should be more favourable since it can be implemented easily on-line without models identified off-line.

3.1. Generalized predictive control

The advanced model-based protocol called GPC is briefly introduced, which requires an underline model (i.e., a prediction model) of the controlled plant

$$A(q^{-1})y(t+1) = B(q^{-1})u(t) + L(q^{-1})\mathbf{d}(t) + \frac{e(t+1)}{\Delta} \tag{2}$$

where

$$\mathbf{d}(t) \triangleq (d_1(t), d_2(t))^T,$$

$$A(q^{-1}) = 1 + a_1q^{-1} + a_2q^{-1} + \cdots + a_{n_a}q^{-n_a},$$

$$B(q^{-1}) = b_0 + b_1q^{-1} + b_2q^{-1} + \cdots + b_{n_b-1}q^{-n_b+1},$$

$$L(q^{-1}) = \mathbf{l}_0 + \mathbf{l}_1q^{-1} + \mathbf{l}_2q^{-1} + \cdots + \mathbf{l}_{n_l-1}q^{-n_l+1},$$

$$\Delta = 1 - q^{-1},$$

and $\mathbf{l}_i \in \mathbb{R}^{1\times 2}$. The control objective is defined as

$$J = (\mathbf{r}-\mathbf{y})^T\mathbf{Q}(\mathbf{r}-\mathbf{y}) + \mathbf{u}^T\mathbf{R}\mathbf{u} \tag{3}$$

where $\mathbf{Q} \in \mathbb{R}^{N_r\times N_r}$, $\mathbf{R} \in \mathbb{R}^{N_r\times N_r}$, and

$$\mathbf{r} = (r(t+1), r(t+2), \ldots, r(t+N_r))^T,$$

$$\mathbf{y} = (\hat{y}(t+1), \hat{y}(t+2), \ldots, \hat{y}(t+N_r))^T,$$

$$\mathbf{u} = (\Delta u(t), \Delta u(t+1), \ldots, \Delta u(t+N_r-1))^T,$$

$$\mathbf{d} = (\mathbf{d}(t)^T, \mathbf{d}(t+1)^T, \cdots, \mathbf{d}(t+N_r-1)^T)^T.$$

Using Diophantine equation [21] iterations, the objective is rewritten as $J = (\mathbf{G}\mathbf{u} + \mathbf{f}' - \mathbf{r})^T\mathbf{Q}(\mathbf{G}\mathbf{u} + \mathbf{f}' - \mathbf{r}) + \mathbf{u}^T\mathbf{R}\mathbf{u}$ where $\mathbf{f}'$ is the filtered responses [21]. The control policy is then derived as

$$\mathbf{u} = (\mathbf{G}^T\mathbf{Q}\mathbf{G} + \mathbf{R})^{-1}\mathbf{G}^T\mathbf{Q}(\mathbf{r} - \mathbf{f}') \tag{4}$$

where only the first row of $\mathbf{u}$ is implemented for the controlled plant. Note that for a model-based protocol, the underline model parameters from sensitivity or identification tests are usually required. For this specific GPC algorithm, the model parameters are $A(q^{-1})$, $B(q^{-1})$ and $L(q^{-1})$ which approximate the PCC plant in some standard mathematical form (Eq. (2)). These model parameters are the indispensable priori knowledge for the model-based control design. To implement the control policy (Eq. (4)), both the matrix $\mathbf{G}$ and the filter $\mathbf{f}'$ should be determined by $A(q^{-1})$, $B(q^{-1})$ and $L(q^{-1})$ beforehand, which infers that GPC is model-based.

3.2. Model-free adaptive control

The PCC process is commonly modelled by first-principle strategies such as equilibrium-based or rate-based approaches [3], which infers that the process involves non-linearities. Note that the time-variant flue gas flow rate, $d_1(t)$ and the mass fraction of CO_2 in flue gas, $d_2(t)$ may cause variations of the process operating point. Thus, non-linearities will lead to mismatches between the controlled plant and the underline model of the model-based controllers, such as GPC. The model-free protocol [14] can form a dynamic linear model on-line for the controlled non-linear plant with a pseudo-partial derivative (PPD) vector $\Phi(t)$. No off-line model parameters are required when the controller is implemented in real time. As the process operating point varies, $\Phi(t)$ adapts to the changes. The control method with $\Phi(t)$ is termed as PFDL which describes the relationship between the input and the output with

$$\Delta y(t+1) = \Phi(t)\Delta\mathbf{U}(t) \tag{5}$$

where

$$\Phi(t) = (\phi_1(t), \phi_2(t)), \cdots, \phi_L(t)) \in \mathbb{R}^{1\times L},$$

$$\Delta\mathbf{U}(t) = (\Delta u(t), \Delta u(t-1), \cdots, \Delta u(t-L+1))^T \in \mathbb{R}^L.$$

$u(t)$, the lean MEA flow rate, is the manipulated input while $y(t)$, the capture level, is the controlled output. When $L = 1$, Eq. (5) is reduced to the CFDL-based description. True $\Phi(t)$ can be estimated by $\hat{\Phi}(t)$ based on the optimisation problem of $J_\Phi = (1/2)\|\hat{\Phi}(t) - \hat{\Phi}(t-1)\|^2$ subject to $\Delta y(t) = \hat{\Phi}(t)\Delta\mathbf{U}(t-1)$ which can be solved by the modified projection algorithm [14]. A control objective is defined as $J_{\mathrm{U}} = \|r(t+1) - y(t+1)\|^2 + \lambda\|\Delta\mathbf{U}(t)\|^2$. By minimizing both J_Φ and J_{U}, the on-line model update is

$$\hat{\Phi}(t) = \hat{\Phi}(t-1) + \frac{\eta(\Delta y(t) - \hat{\Phi}(t-1)\Delta\mathbf{U}(t-1))\Delta\mathbf{U}^T(t-1)}{\mu + \|\Delta\mathbf{U}(t-1)\|^2} \tag{6}$$

and the control policy update is

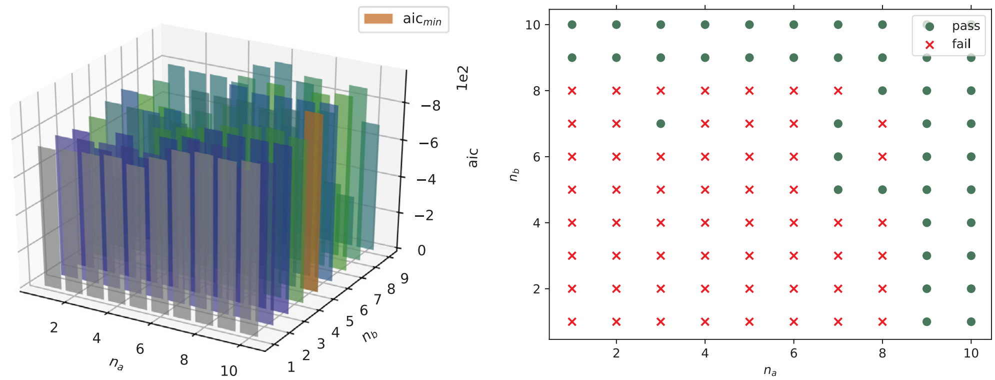

(a) AIC values. (b) Whiteness and independence test.

Fig. 3. Model order searching results.

$$u(t) = u(t-1) + \frac{\rho_1\hat{\phi}_1(t)(r(t+1)-y(t))}{\lambda + |\hat{\phi}_1(t)|^2} - \frac{\hat{\phi}_1(t)\sum_{m=2}^{L}\rho_m\hat{\phi}_m(t)\Delta u(t-m+1)}{\lambda + |\hat{\phi}_1(t)|^2} \tag{7}$$

where $\hat{\Phi}(t) = (\hat{\phi}_1(t), \hat{\phi}_2(t)), \cdots, \hat{\phi}_L(t)) \in \mathbb{R}^{1\times L}$ and $r(t+1)$ is the set-point of the output. For stability of the closed-loop system, the reset rule is

$$\hat{\phi}_1(t) = \hat{\phi}_1(1), \text{ if } |\hat{\phi}_1(t)| < b \text{ or } |\hat{\phi}_1(t)| > \alpha b \text{ or } \mathrm{sign}(\hat{\phi}_1(t)) \neq \mathrm{sign}(\hat{\phi}_1(1)). \tag{8}$$

Eqs. (6)–(8) form the iterative algorithm of the MFAC protocol [13]. To apply this algorithm, tuning parameters within constraints (i.e., $\eta \in (0,1), \mu > 0, \boldsymbol{\rho} = (\rho_1, \rho_2, \cdots, \rho_L)^T$ with $\rho_m \in (0,1)$ for any $m, \lambda > \lambda_{\min} > 0, \alpha > 1$, and $b > 0$) should be determined by the user. η and μ are related to the adaptive performances of the dynamic linear model for the controlled PCC plant. $\boldsymbol{\rho}$ and λ are related to the control performances for the plant. For fast responses, η and $\boldsymbol{\rho}$ should be increased while for smooth dynamics, μ and λ should be increased. The PPD vector $\hat{\Phi}(t)$ is updated on-line without using any prior knowledge of the off-line model, which implies the iterative algorithm is model-free. Arbitrary initial conditions of $\hat{\Phi}(t=1)$ should be specified to set up the iteration.

Compared with PI control, the above iterative method is easy to guarantee stability. If the closed-loop system is unstable or marginally stable, only the stabilizing parameter λ should be increased for the stabilization while PI control requires stability analysis such as the Nyquist criterion to determine whether to increase or decrease tuning parameters. In addition, the Nyquist criterion is a model-based method requiring model parameters. Furthermore, PI control is generally designed around fixed operating points while MFAC forms an adaptive dynamic linear model using on-line model update (Eq. (6)), i.e., MFAC already considers model uncertainties and should have strong robustness.

Compared with GPC requiring a prediction model, MFAC can be easily tuned on-line with measured input–output data of the controlled plant. If the underline model is inaccurate, the performances of GPC will be deteriorated. For the PCC process which is sensitive to ambient environments and is non-linear, a large number of sensitivity or identification tests should be conducted around different operating points of the controlled plant before the controller can be applied on-line. MFAC only uses input–output data of the PCC plant. No off-line model parameters are necessary for the on-line control implementation. The identified mathematical model of the PCC process is only used for the initial off-line tuning. Afterwards, if the control performance is unsatisfactory, MFAC can be retuned on-line [13] without off-line models. However, if the control performance of a model-based controller is poor, the model may be re-identified off-line based on new data generated by the first-principle model, which is non-trivial. Therefore, the implementation of MFAC is easier.

4. Simulation results

4.1. Identification of a carbon capture plant model with neural networks

The observed data for the plant model identification are generated by the first-principle PCC model [17] with the sampling time $T_s = 2.5$ s. During preprocessing, dc-offsets of both the input features $\mathbf{x}(t)$ and output $y(t)$ are removed. The model structure is a neural network with an unknown hidden layer size and model orders, both reflected by D_0, the total number of model parameters. In Section 4.1, D_0 is determined by n_a, n_b, n_{d1}, n_{d2} and H. To reduce the number of candidate models, $n_b = n_{d1} = n_{d2}$ with the hidden layer size $H = 1$ is assumed for the initial model order selection. Only n_a and n_b should be determined to fix D_0. For both n_a and n_b ranging from 1 to 10, the model performances are quantized by AIC. Theoretically, the selected model orders should have the minimum AIC value (Fig. 3a), i.e., $n_a = 10$ and $n_b = 5$. The model order pair selected by Akaike's information criterion with a correction for finite sample sizes (AIC$_c$) or Bayesian information criterion (BIC) [20] is $n_a = 5$ and $n_b = 5$.

Correspondingly, the selected candidate models must pass the whiteness and independence tests so as to validate their performances on approximating the first principle PCC model [17]. The tests are conducted not only for the models selected by AIC, AIC$_c$ or BIC, but the candidate models with orders around the neighbours of the criterion-based ones, i.e., n_a and n_b are searched within $\{1, 2, 3, 4, 5, 6, 7, 8, 9, 10\}$. The hidden layer size H is enumerated from 1 to 10. For each specified H and n_a-n_b pair, a validated model must meet two constraints: (a) It can achieve a good fit (over 90% fit) with the observed data generated by the first-principle model; (b) the residual $\epsilon(t)$ of the candidate model can pass whiteness and independence tests. If there exists any H such that the whiteness and independence tests are passed, this n_a-n_b pair is recorded with "pass" (Fig. 3b). Although the model order pair, $n_a = 5$ and $n_b = 5$, is selected by AIC$_c$ or BIC, the corresponding candidate model fails the tests (Fig. 3b). Table 1 only gives the smallest hidden layer sizes $H_{\min}$ with respect to some typical model order pairs (determined by AIC, AIC$_c$, BIC, etc.) such that the candidate models can

Table 1
Validated model orders and fit percentages.

(n_a, n_b)	$H_{\min}$	fit (%)
(5,5)	/	/
(7,5)	3	97.77
(10,1)	1	98.41
(10,5)	1	98.42

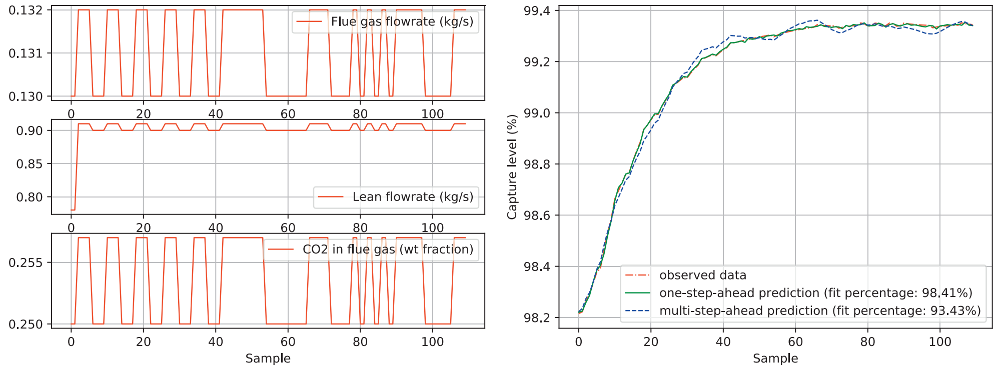

(a) Input dynamics. (b) Output dynamics.

Fig. 4. Comparison between the first-principle and neural network models.

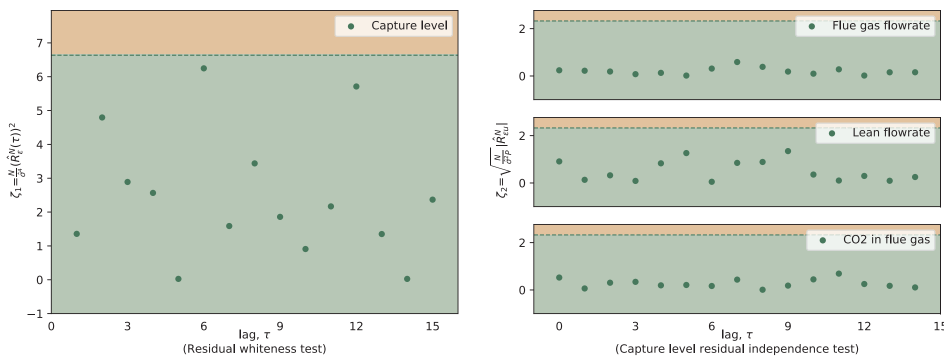

(a) The whiteness test. (b) The independence test.

Fig. 5. Residual analysis with 99% confidence level.

pass the whiteness and independence tests. It is observed that if the model has passed the tests, the fit percentage is generally over 90%. Instead of the above constraints for validated models, the number of model parameters D_0 is further considered to avoid over-fitting. A candidate model with $n_a = 10$, $n_b = 1$, and $H_{\min} = 1$ is finally selected since $D_0 = (n + 2)\cdot H + 2 = 17$ is the smallest among all the validated models. The selected model should have the one-step-ahead structure (Eq. (1)) since the control protocols are based on one-step-ahead algorithms (Eqs. (4) and (7)). According to input and output dynamics (Fig. 4), the fit percentage of the selected model is 98.41% for the one-step-ahead prediction. Furthermore, the selected model also has reasonable performance on the multi-step-ahead prediction. The fit percentage for the carbon capture level is 93.43%. This value is lower than 98.41% of the one-step-ahead prediction but still well above 90%. The residual analysis (Fig. 5) of the model indicates $\zeta_1(\tau)$ and $\zeta_2(\tau)$ are within the 99% confidence intervals.

4.2. Model-free adaptive controller design

The performances of CFDL- and PFDL-MFAC are evaluated based on the previous validated non-linear PCC plant model, i.e., the controlled plant in the subsequent sections. PI control results are also given for comparisons. The lean MEA flow rate is the manipulated input while the carbon capture level is the controlled output. The original controlled plant is supposed to be free of disturbances. During the tuning process, K_p and K_i (Table 2) of PI control [17] are tuned to ensure tracking performances of the capture level as best as possible. Then, instead of PI control, MFAC can be tuned as discussed in Section 3.2 and implemented to achieve similar performances (Fig. 6a) with the designed tuning parameters (Table 2). Although the number of tuning parameters for MFAC is larger than that for PI control, MFAC is easy to ensure stability [14]. PI control needs extra stability analysis of the

Table 2
Controller design.

	PI		CFDL-MFAC	PFDL-MFAC
K_p	0.01	μ	0.002	0.002
K_i	0.017	λ	25	40
		ρ	(1)	$(0.8, 0.05, 0.001)^T$
		α	200	200
		η	0.4	0.4
		b	0.1	0.1
		L	1	3
		$\hat{\Phi}(1)$	(3)	$(3, -5, -2)$

closed-loop system.

Afterwards, the time-variant disturbances, i.e., the flue gas flow rate and the CO_2 mass fraction of the flue gas (Fig. 7), are applied to the controlled non-linear PCC plant, which can be periodical ramp changes due to the variations of power generation [4]. Simultaneously, the reference signal of the carbon capture level is generated identically to the one of the undisturbed system (Fig. 6a). Based on the previous tuning parameters (Table 2), only the capture level deviations from the references (Fig. 6b) are plotted, where PFDL-MFAC has the smoothest transient responses of the output, i.e. the smallest carbon capture level deviations than the PI control and CFDL-MFAC algorithms. PFDL-MFAC is better (Fig. 6b) than CFDL, since time-variant PPD $\hat{\Phi}(t)$ of PFDL with a longer length $L = 3$ (Table 2) adaptively catches more system dynamics. CFDL-MFAC with fewer tuning parameters than PFDL-MFAC, however, can be designed more easily for simple plants [14]. Both CFDL- and PFDL-MFAC can guarantee stability by increasing the stabilizing parameter λ. Time-variant $\hat{\Phi}(t)$ for CFDL and PFDL (Fig. 8) dynamically estimate the controlled non-linear plant.

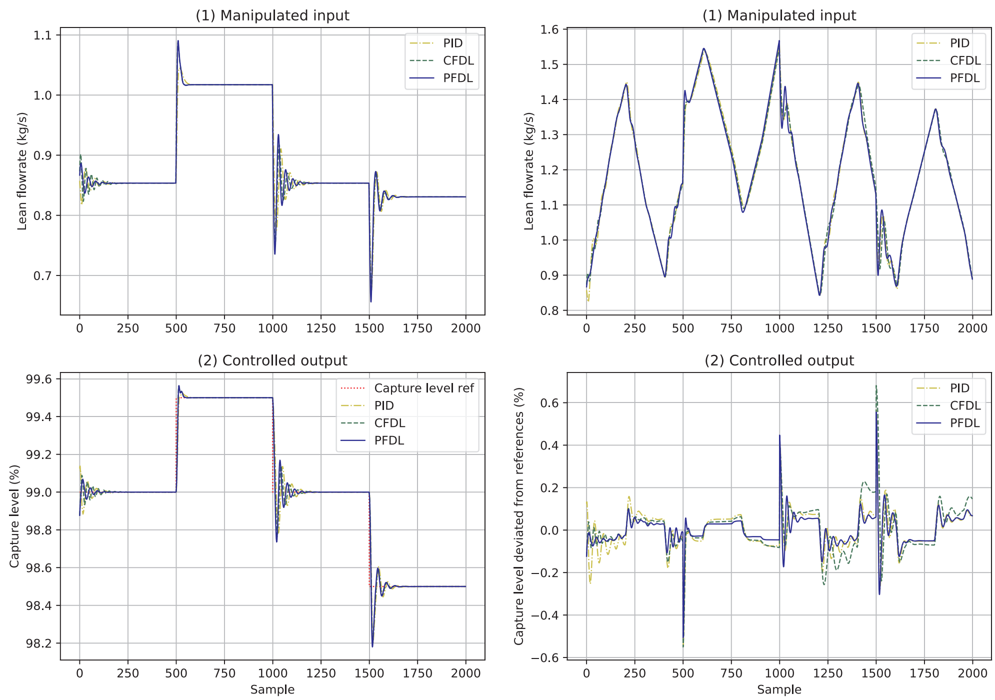

(a) The undisturbed closed-loop system. (b) The disturbed closed-loop system.

Fig. 6. MFAC and PI control results.

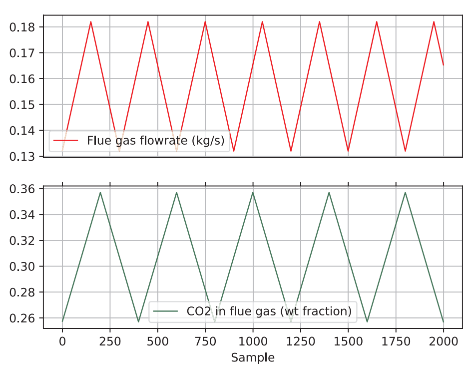

Fig. 7. Disturbances.

4.3. Comparison between model-based and model-free controllers

PFDL-MFAC is compared with GPC in this section. Note that the controlled non-linear PCC plant is the validated neural network selected in Section 4.1. The prediction model (Eq. (2)) is linearised based on this non-linear plant using the first-order Taylor approximation so as to derive $A(q^{-1})$, $B(q^{-1})$ and $D(q^{-1})$. These polynomials inevitably generate model uncertainties due to plant non-linearities. For the same input dynamics (Fig. 4a), there exist mismatches between the output responses of the prediction model, the controlled non-linear plant and the first-principle model (Fig. 9a). Based on the prediction model, to implement the GPC algorithm, the time horizon N_r, and the weight matrices $\mathbf{Q}$ and $\mathbf{R}$ in the control objective (Eq. (3)) should be determined by the user. N_r is the concerned time horizon. $\mathbf{Q}$ is the penalty of the tracking error (i.e., $r(t+k)-y(t+k)$) within the time horizon N_r. $\mathbf{R}$ is the penalty of the manipulated input deviation (i.e., $\Delta u(t+k) = u(t+k)-u(t+k-1)$) within the time horizon N_r. The control objective (Eq. (3)) indicates there should be trade-off between the tracking error and the input manipulation. For the smooth input dynamics, entries of $\mathbf{Q}$ should be large while those of $\mathbf{R}$ should be small. In contrast, for the fast output responses, entries of $\mathbf{Q}$ should be small while those of $\mathbf{R}$ should be large. In this case study, the best performance of GPC is obtained with the tuning parameters of

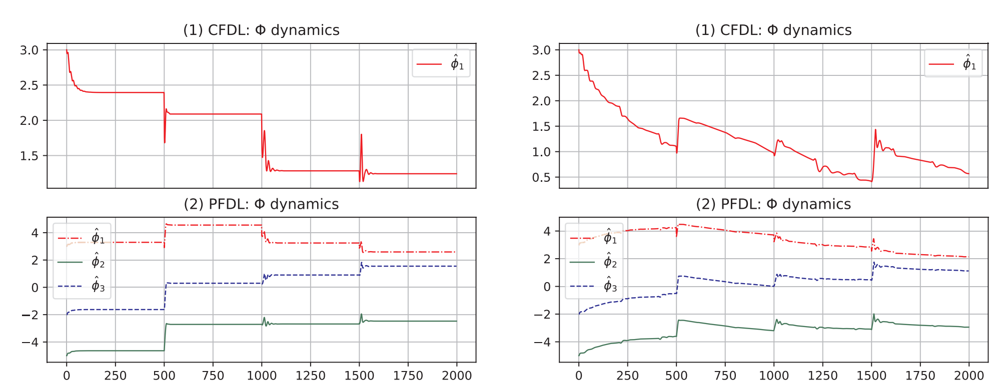

(a) $\hat{\Phi}(t)$ dynamics for the undisturbed system. (b) $\hat{\Phi}(t)$ dynamics for the disturbed system.

Fig. 8. PPD vector dynamics.

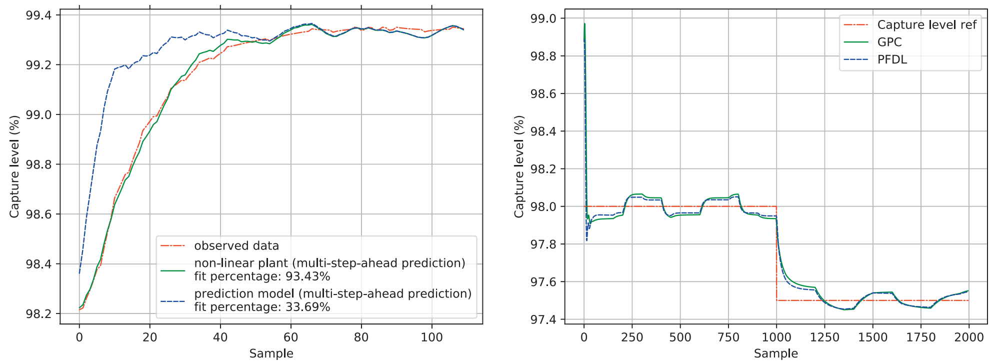

(a) Output of the first-principle model, non-linear plant, and prediction model.

(b) Tracking performances of model-based and model-free controllers.

Fig. 9. GPC and PFDL-MFAC results.

$N_r = 3$,$\mathbf{Q} = 1 \cdot I_{N_r \times N_r}$ and $\mathbf{R} = 30 \cdot I_{N_r \times N_r}$ where $I_{N_r \times N_r} \in \mathbb{R}^{N_r \times N_r}$ is an identity matrix. Simultaneously, Fig. 9b shows PFDL-MFAC achieves a similar tracking performance as GPC. Nevertheless, an underline model should be identified before the tuning parameters of GPC can be tested on-line. The model not only lacks non-linearities of the controlled plant but is usually obtained with off-line sensitivity or identification tests. Both of them make the tuning procedure more complex than MFAC.

5. Conclusions

We have identified a validated non-linear PCC plant model using the data generated by a first-principle model. The candidate models are approximately located by model order selection criteria such as AIC, AIC_c and BIC, and then searched around the neighbours of the criterion-determined model orders. The plant model can pass residual analysis and fit well with the data set.

We have implemented the PI control and the model-free algorithms, namely, CFDL- or PFDL-MFAC within the validated non-linear PCC plant model. PFDL-MFAC has shown the best performance when confronting model uncertainties caused by time-variant disturbances. CFDL-MFAC, however, can be tuned easily since it has fewer tuning parameters. Both CFDL- and PFDL-MFAC can guarantee the stability of the closed-loop system by the stabilizing parameter λ, easier than PI control using the model-based Nyquist criterion.

We have compared PFDL-MFAC with a model-based method called GPC. PFDL-MFAC can be more flexibly tuned on-line without model parameters determined during the off-line system identification. GPC, however, must be applied based on underline models, which is linearised around specified equilibrium points of the controlled non-linear plant. Extra time should be taken to ensure the model performances. When performances of such a model-based controller are unsatisfactory, re-identification of underline models may be required, which is non-trivial. Consequently, PFDL-MFAC can be flexibly designed and implemented easily on-line with a simplified off-line tuning process.

References

[1] Lawal A, Wang M, Stephenson P, Yeung H. Dynamic modelling of CO_2 absorption for post combustion capture in coal-fired power plants. Fuel 2009;88(12):2455–62.
[2] Bui M, Gunawan I, Verheyen V, Feron P, Meuleman E, Adeloju S. Dynamic modelling and optimisation of flexible operation in post-combustion CO_2 capture plants-A review. Comput Chem Eng 2014;61(Supplement C):245.
[3] Wang M, Lawal A, Stephenson P, Sidders J, Ramshaw C. Post-combustion CO_2 capture with chemical absorption: a state-of-the-art review. Chem Eng Res Des 2011;89(9):1609–24.
[4] Lawal A, Wang M, Stephenson P, Obi O. Demonstrating full-scale post-combustion CO_2 capture for coal-fired power plants through dynamic modelling and simulation. Fuel 2012;101(Supplement C):115–28.
[5] Li Z, Ding Z, Wang M. Operation and bidding strategies of power plants with carbon capture. IFAC-Papers OnLine 2017;50(1):3244–9. 20th IFAC World Congress.
[6] Nittaya T, Douglas PL, Croiset E, Ricardez-Sandoval LA. Dynamic modelling and control of MEA absorption processes for CO_2 capture from power plants. Fuel 2014;116(Supplement C):672–91.
[7] Lin YJ, Wong DSH, Jang SS, Ou JJ. Control strategies for flexible operation of power plant with CO_2 capture plant. AIChE J 2012;58(9):2697–704.
[8] Arce A, Mac Dowell N, Shah N, Vega LF. Flexible operation of solvent regeneration systems for CO_2 capture processes using advanced control techniques: Towards operational cost minimisation. Int J Greenhouse Gas Control 2012;11:236–50. Complete.
[9] Sahraei MH, Ricardez-Sandoval L. Controllability and optimal scheduling of a CO_2 capture plant using model predictive control. Int J Greenhouse Gas Control 2014;30(Supplement C):58–71.
[10] Peng J, Edgar TF, Eldridge RB. Dynamic rate-based and equilibrium models for a packed reactive distillation column. Chem Eng Sci 2003;58(12):2671–80.
[11] Hou ZS, Wang Z. From model-based control to data-driven control: survey, classification and perspective. Inf Sci 2013;235:3–35.
[12] Ljung L. System Identification: theory for the user. PTR Prentice Hall Information and System Sciences Series; 1987.
[13] Hou Z, Jin S. Data-driven model-free adaptive control for a class of MIMO nonlinear discrete-time systems. IEEE Trans Neural Networks 2011;22(12):2173–88.
[14] Hou Z, Jin S. A novel data-driven control approach for a class of discrete-time nonlinear systems. IEEE Trans Control Syst Technol 2011;19(6):1549–58.
[15] Dugas RE. Pilot plant study of carbon dioxide capture by aqueous monoethanolamine [Ph.D. thesis]; 2006.
[16] Li Z, Ding Z, Wang M. Optimal bidding and operation of a power plant with solvent-based carbon capture under a CO_2 allowance market: a solution with a reinforcement learning-based sarsa temporal-difference algorithm. Engineering 2017;3(2):257–65.
[17] Biliyok C, Lawal A, Wang M, Seibert F. Dynamic modelling, validation and analysis of post-combustion chemical absorption CO_2 capture plant. Int J Greenhouse Gas Control 2012;9:428–45.
[18] Sipcz N, Tobiesen FA, Assadi M. The use of artificial neural network models for CO_2 capture plants. Appl Energy 2011;88(7):2368–76.
[19] Li F, Zhang J, Oko E, Wang M. Modelling of a post-combustion CO_2 capture process using neural networks. Fuel 2015;151(Supplement C):156–63.
[20] Burnham KP, Anderson DR. Model selection and multimodel inference: a practical information-theoretic approach. Springer Science & Business Media; 2002.
[21] Camacho EF, Alba CB. Model predictive control. Springer Science & Business Media; 2013.